

**NUCLEAR DATA AND MEASUREMENTS SERIES**

**ANL/NDM-14**

**Cross Sections for the  $^{66}\text{Zn}(n,p)^{66}\text{Cu}$ ,  $^{113}\text{In}(n,n')^{113\text{m}}\text{In}$ , and  
 $^{115}\text{In}(n,n')^{115\text{m}}\text{In}$  Reactions  
from Near Threshold to 10 MeV**

by

Donald L. Smith and James W. Meadows

July 1975

**ARGONNE NATIONAL LABORATORY,  
ARGONNE, ILLINOIS 60439, U.S.A.**

# NUCLEAR DATA AND MEASUREMENTS SERIES

ANL/NDM-14

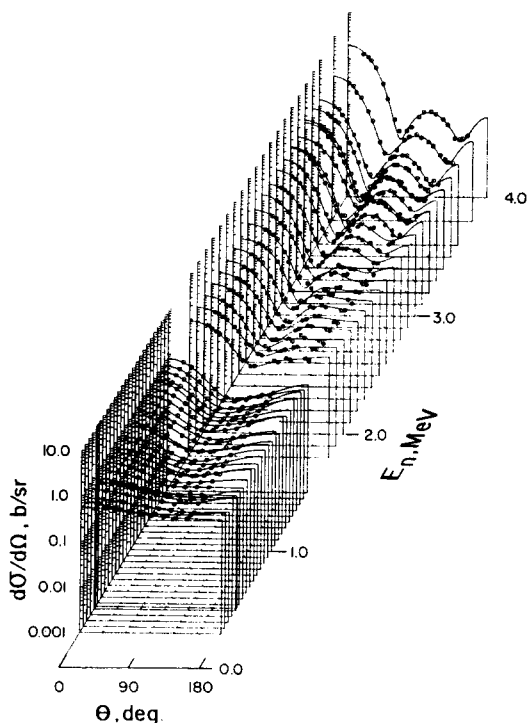
Cross Sections for the  $^{66}\text{Zn}(n,p)^{66}\text{Cu}$ ,  
 $^{113}\text{In}(n,n')^{113\text{m}}\text{In}$  and  $^{115}\text{In}(n,n')^{115\text{m}}\text{In}$

Reactions from Near Threshold to 10 MeV

by

Donald L. Smith and James W. Meadows

July 1975



U of C - AUA - USAEC

ARGONNE NATIONAL LABORATORY,  
ARGONNE, ILLINOIS 60439, U.S.A.

The facilities of Argonne National Laboratory are owned by the United States Government. Under the terms of a contract (W-31-109-Eng-38) between the U. S. Atomic Energy Commission, Argonne Universities Association and The University of Chicago, the University employs the staff and operates the Laboratory in accordance with policies and programs formulated, approved and reviewed by the Association.

#### MEMBERS OF ARGONNE UNIVERSITIES ASSOCIATION

The University of Arizona	Kansas State University	The Ohio State University
Carnegie-Mellon University	The University of Kansas	Ohio University
Case Western Reserve University	Loyola University	The Pennsylvania State University
The University of Chicago	Marquette University	Purdue University
University of Cincinnati	Michigan State University	Saint Louis University
Illinois Institute of Technology	The University of Michigan	Southern Illinois University
University of Illinois	University of Minnesota	The University of Texas at Austin
Indiana University	University of Missouri	Washington University
Iowa State University	Northwestern University	Wayne State University
The University of Iowa	University of Notre Dame	The University of Wisconsin

#### NOTICE

This report was prepared as an account of work sponsored by the United States Government. Neither the United States nor the United States Atomic Energy Commission, nor any of their employees, nor any of their contractors, subcontractors, or their employees, makes any warranty, express or implied, or assumes any legal liability or responsibility for the accuracy, completeness or usefulness of any information, apparatus, product or process disclosed, or represents that its use would not infringe privately-owned rights.

ANL/NDM-14

Cross Sections for the  $^{66}\text{Zn}(n,p)^{66}\text{Cu}$ ,  
 $^{113}\text{In}(n,n')^{113\text{m}}\text{In}$  and  $^{115}\text{In}(n,n')^{115\text{m}}\text{In}$

Reactions from Near Threshold to 10 MeV

by

Donald L. Smith and James W. Meadows

July 1975

In January 1975, the research and development functions of the former U.S. Atomic Energy Commission were incorporated into those of the U.S. Energy Research and Development Administration.

Applied Physics Division  
Argonne National Laboratory  
9700 South Cass Avenue  
Argonne, Illinois 60439  
U.S.A.

## NUCLEAR DATA AND MEASUREMENTS SERIES

The Nuclear Data and Measurements Series presents results of studies in the field of microscopic nuclear data. The primary objective is the dissemination of information in the comprehensive form required for nuclear technology applications. This Series is devoted to: a) Measured microscopic nuclear parameters, b) Experimental techniques and facilities employed in data measurements, c) The analysis, correlation and interpretation of nuclear data, and d) The evaluation of nuclear data. Contributions to this Series are reviewed to assure technical competence and, unless otherwise stated, the contents can be formally referenced. This Series does not supplant formal journal publication but it does provide the more extensive information required for technological applications (e.g., tabulated numerical data) in a timely manner.

## TABLE OF CONTENTS

	<u>Page</u>
ABSTRACT . . . . .	3
1. INTRODUCTION . . . . .	4
2. EXPERIMENTAL PROCEDURE . . . . .	7
2.1. General Measurement Procedure . . . . .	7
2.2. Data Processing and Error Analysis. . . . .	9
2.3. $^{66}\text{Zn}(n,p)^{66}\text{Cu}$ Measurements. . . . .	11
2.4. $^{113,115}\text{In}(n,n')^{113m,115m}\text{In}$ Measurements . . . . .	11
3. EXPERIMENTAL RESULTS AND DISCUSSION. . . . .	12
3.1. $^{66}\text{Zn}(n,p)^{66}\text{Cu}$ Reaction. . . . .	12
3.2. $^{113,115}\text{In}(n,n')^{113m,115m}\text{In}$ Reactions . . . . .	12
4. EYEGUIDES FOR EXPERIMENTAL DATA. . . . .	13
5. RESPONSE IN REFERENCE FISSION NEUTRON FIELDS . . . . .	14
REFERENCES . . . . .	16
TABLES . . . . .	18
FIGURES. . . . .	32

CROSS SECTIONS FOR THE  $^{66}\text{Zn}(n,p)^{66}\text{Cu}$ ,  
 $^{113}\text{In}(n,n')^{113\text{m}}\text{In}$  and  $^{115}\text{In}(n,n')^{115\text{m}}\text{In}$   
REACTIONS FROM NEAR THRESHOLD TO 10 MEV\*

by

Donald L. Smith and James W. Meadows

ABSTRACT

Activation techniques were used in the measurement of cross sections for the  $^{66}\text{Zn}(n,p)^{66}\text{Cu}$ ,  $^{113}\text{In}(n,n')^{113\text{m}}\text{In}$  and  $^{115}\text{In}(n,n')^{115\text{m}}\text{In}$  reactions from near threshold to 10 MeV. The  $^7\text{Li}(p,n)^7\text{Be}$  and  $\text{D}(d,n)^3\text{He}$  reactions were employed as sources of approximately monoenergetic neutrons. Neutron fluence was measured with a fission chamber which contained calibrated uranium deposits enriched in  $^{235}\text{U}$  or  $^{238}\text{U}$ . Gamma-ray activities of the irradiated samples were measured with  $\text{NaI}(\text{Tl})$  scintillation and  $\text{Ge}(\text{Li})$  detectors. The raw data were corrected for various experimental effects including activity decay, detector efficiencies, geometry, absorption, multiple scattering, internal conversion, deadtime, sum coincidences, and sample and uranium deposit properties. The response of the monoenergetic cross section data in reference neutron fields characteristic of thermal fission of  $^{235}\text{U}$  and spontaneous fission of  $^{252}\text{Cf}$  was numerically investigated. The results of our work are compared with corresponding information reported in the literature.

\*This work performed under the auspices of the U.S. Energy Research and Development Administration.

## 1. INTRODUCTION

Many neutron-induced reactions which are important for various nuclear applications can be investigated through measurement of the activities of the reaction products. Some reactions exhibit characteristic thresholds, cross sections, emission radiations and decay half lives which qualify them for use as monitors in fast-neutron dosimetry. Other reactions are important for analysis of radiation damage in high-fluence neutronic systems. In spite of their importance for applications, the cross sections for many of these reactions are not well known and requests for improved data can be found in several documents [1-3].

Measurements of cross sections for reactions of this nature have been in progress at Argonne National Laboratory for several years; this program gained momentum in 1970 when the ANL Tandem Dynamitron accelerator facility (Fast-Neutron Generator) became available for Fast-Neutron Physics research [4]. Results from this work and detailed descriptions of the experimental method have been reported (e.g., Refs. 5-10). The objective of this report is to present the results of recent measurements on the  $^{66}\text{Zn}(n,p)^{66}\text{Cu}$ ,  $^{113}\text{In}(n,n')^{113\text{m}}\text{In}$  (99.4m) and  $^{115}\text{In}(n,n')^{115\text{m}}\text{In}$  (4.5h) reactions for energies from near threshold to  $\sim 10$  MeV. Very little data is available on the first two reactions and the results of the present work provide a significant improvement in knowledge of their cross sections for this energy region. Considerable data is available for the  $^{115}\text{In}(n,n')^{115\text{m}}\text{In}$  (4.5h) reaction. Our results are in substantial agreement with these data.

Several factors make it feasible to improve the knowledge of fast-neutron activation cross section data at this time:

- a. Accelerators with wide energy ranges and large beam intensities (e.g., the FNG can provide 150-200  $\mu$ A of protons or deuterons with any desired energy in the range 1.5 - 8 MeV) are now available (a major limitation is heat dissipation by the target).
- b. Modern Ge(Li) detectors enable measurement of gamma-ray activities with precision, selectivity and considerable efficiency.
- c. Remarkable progress has been made during recent years in improving the knowledge of decay parameters (half-lives, decay schemes, etc.) for most radioactive nuclides.
- d. Improved experimental and theoretical techniques have expanded our knowledge of internal conversion parameters.
- e. The properties of common neutron sources such as the  ${}^7\text{Li}(p,n){}^7\text{Be}$ ,  $\text{D}(d,n){}^3\text{He}$ ,  $\text{T}(p,n){}^3\text{He}$  and  $\text{T}(d,n){}^4\text{He}$  reactions are now reasonably well known as the result of recent experimental studies and evaluations.
- f. Modern digital computers enable more accurate analysis of experimental data and the application of corrections which were previously impractical.

In spite of this potential for improvement of the data base, there are few active experimental programs underway in this area. Also worthy of mention is the fact that theoretical advances in the area of neutron activation reactions have been limited. Most of the effort has been directed to the region around 14 MeV (probably because of the abundance of data available near this energy). More comprehensive theoretical effort, encompassing wide ranges of neutron energy, atomic number (Z) and mass number (A),

is desirable because experimental programs may not be capable of providing needed results, in certain unfavorable cases, early enough to satisfy requirements for some important applications [11].

We chose to employ the fission of  $^{235}\text{U}$  and  $^{238}\text{U}$  as neutron fluence monitors for our measurements at energies below 10 MeV. A few words in support of this method are appropriate since it is more common to rely on methods which utilize the n-p scattering process (a standard). Experimenters who employ the n-p scattering process must contend with severe technical difficulties in order to obtain accurate results (especially at low energies) even though the cross section is well known. Two key problems are, i) the difficulty in distinguishing low-energy recoil protons from electronic noise, and ii) the determination of the absolute number of hydrogen atoms in the detectors. Fission detectors are more convenient. The uranium deposit masses can be determined to  $\sim 1\%$  and the isotopic fractions can be measured with even greater accuracy [10, 12]. The largest source of uncertainty is in the fission cross sections. As a result of recent efforts in this area, these cross sections are probably known to within  $\sim 5\%$  for the neutron energies considered in this work. Since this accuracy exceeds that which we expect to achieve in most activation measurements, we consider these fission reactions to be suitable fluence monitors for these measurements.

We measured the ratios of activation cross sections to fission cross sections. Therefore, our basic data are presented in this form. We also computed cross sections based on current standard values for the monitor reactions (i.e., the ENDF/B-IV [13] fission cross sections). A sufficient number of values were selected from the ENDF/B-IV files to adequately represent the monitor cross sections in

the region of interest for our work (see Table I).

We constructed eyeguides through plots of the cross sections. Points were selected from the eyeguides and these are also presented in this report. The eyeguide cross sections adequately represent the principal features of our data while avoiding the ambiguities of experimental values. The eyeguide curves were then used to test the response of our data in reference neutron spectra for comparison with some reported integral parameters.

## 2. EXPERIMENTAL PROCEDURE

The experimental method is described in detail in earlier reports [5,8,9]. Highlights of the general method and specific details relevant to the reactions under investigation are presented in this section.

### 2.1. General Measurement Procedure

Samples of high-purity natural metals in the form of 2.54-cm dia by 0.16-0.32 cm thick disks were employed for the measurements. The materials used to fabricate these samples were analyzed by spectrochemical methods to determine the impurities content. No significant impurities were found in any of the samples.

During irradiation, each sample was fastened to a low-mass fission detector which served as the neutron-fluence monitor [14]. This ionization chamber was made from a cylindrical steel can with 0.025-cm-thick walls. The samples were placed outside the chamber; the backing plates with uranium deposits were mounted inside the chamber adjacent to the samples, as shown in Fig. 1. Methane at 1 atm served as the gaseous medium for the ionization chamber. A discriminator was used to reject noise and alpha pulses; pulses above the discrimination level were recorded as fission events in the detector.

The uranium deposits were 2.54cm in diameter and were fabricated by evaporating  $UF_4$  isotopically enriched in  $^{235}U$  or  $^{238}U$  onto thin, metal backing plates. The isotopic contents of these materials were determined by mass spectrographic analysis; the quantity of uranium in each deposit was deduced from measurements of the specific alpha activities [5,9,10]. The masses of fissionable-material deposits used in the fission detector were in the range 0.5-5 milligrams. The deposits enriched in  $^{235}U$  were used for measurements with  $E_n < 3$  MeV; deposits enriched in  $^{238}U$  were used for measurements with  $E_n \geq 3$  MeV in order to minimize the corrections for low-energy neutrons.

Neutrons with energies in the range 0.4-5.8 MeV were produced via the  $^7Li(p,n)^7Be$  reaction (proton-energy range 2.15-7.5 MeV). Natural lithium metal was evaporated onto tantalum cups to make these targets. Neutrons with energies in the range 5-10.1 MeV were produced via the  $D(d,n)^3He$  reaction (deuteron energy range 1.8-6.9 MeV). A 2-cm-long gas cell containing deuterium gas at 2 atm (see Fig. 1) was used for a target. The sample and fission detector were placed on the beam axis 3 to 6 cm from the target for these measurements (see Fig. 1). There are variations in the experimental techniques associated with use of these two types of targets. The neutron spectrum from the lithium target is complex at higher energies because of the presence of neutrons from the  $^7Li(p,n)^7Be^*$  and  $^7Li(p,n^3He)^4He$  reactions. The presence of neutrons from the  $D(d,np)D$  reaction complicates the neutron spectrum from the deuterium source at higher energies. Methods for coping with these problems have been reported [5,8,15]. Background measurements were performed during irradiations made using both lithium and deuterium targets to determine the effects of neutrons from the tantalum cups and empty gas-target assembly respectively.

The activities of irradiated samples were measured using standard gamma-ray counting techniques. Most of the

counting was done using a Ge(Li) detector (Fig. 2); however, the zinc samples were counted with a NaI(Tl) scintillation detector. The relative gamma-ray full-energy peak efficiency vs. energy was measured for each detector using a method described by Freeman and Jenkin [16]. The absolute efficiency of each detector was determined at 0.811 and 1.274 MeV by counting  $^{58}\text{Co}$  and  $^{22}\text{Na}$  standard sources respectively; the absolute activities of these standards were determined by coincidence-counting techniques.

## 2.2 Data Processing and Error Analysis

Cross sections for the reactions studied were computed relative to  $^{235}\text{U}$  and  $^{238}\text{U}$  fission cross sections after correcting the data for various experimental effects. Properties of the target- and reaction-product nuclei, which were required for these computations, were obtained from various data compilations; the pertinent parameters are presented in Table II [17-21].

Corrections for neutron-source properties were deduced from data obtained from measurements made at our own laboratory [5,8,15] and from a paper by Liskien and Paulsen [22]. The raw data were corrected, where required, for sample activity and monitor fissions produced by neutrons from bare target assemblies. Corrections were made to account for geometric factors and the effects of neutron absorption and multiple scattering (Fig. 3). Raw fission counts were corrected for deposit-thickness effects, thermal background (for  $^{235}\text{U}$  monitors) and loss of low-pulse-height fission events rejected along with electronic noise and alpha pulses by a discriminator.

Raw sample-count data were corrected for decay half life and other essential time factors. Corrections were also applied to account for specific decay properties of the

product nuclei, detector efficiency, counting geometry, deadtime losses, gamma-ray absorption, and coincidence-summing losses. Monte-Carlo calculations were made to correct the data for differences in counting efficiencies resulting from absorption and geometric factors. Corrections for internal conversion were deduced from information available in a paper by Hager and Seltzer [20].

Table III summarizes the corrections applied to the experimental data. The application of various corrections and computation of reaction cross sections were carried out for the most part with the aid of a digital computer. Therefore, it was possible to investigate in detail the sensitivity of the computed cross sections to the various applied corrections.

The energy resolution for these measurements was governed by target thickness and kinematic broadening. Kinematic broadening was the dominant factor in measurements with the deuterium-gas target. Generally, the neutron-energy resolution was 0.04-0.15 MeV for the lithium target measurements and 0.3-0.4 MeV for deuterium-target measurements.

Uncertainties in the measured cross sections can be attributed to statistics as well as a variety of other experimental factors. Known systematic uncertainties amounted to  $\sim 6\%$  for these measurements. This was combined with the statistical uncertainties in quadrature in order to obtain the total reported errors for the measured cross sections. Uncertainties in the fission cross sections, the internal conversion coefficients and decay-branching factors were not included in the assigned error bars. We relied on computed or evaluated values from the literature, and our measured results could be adjusted to accommodate any future revisions in these

parameters. Table IV indicates the relative importance of some of the identified sources of uncertainty in our data. Statistical uncertainties were relatively unimportant except for measurements near thresholds.

### 2.3. $^{66}\text{Zn}(n,p)^{66}\text{Cu}$ Measurements

The natural abundance of  $^{66}\text{Zn}$  is 27.81% [17] and this reaction has a Q-value of -1.852 MeV [18].  $^{66}\text{Cu}$  decays with a half life of 5.10 m through  $\beta^-$  emission to levels in  $^{66}\text{Zn}$ . Most of the decays proceed via a transition to the ground state; however, there are 9 gamma rays of 1.033 MeV produced for every 100  $^{66}\text{Cu}$  decays [19]. These gamma rays were detected and their yield was utilized in determination of the reaction cross section. The correction for coincidence summing was negligibly small. Internal-conversion effects were also very small [20].

### 2.4. $^{113,115}\text{In}(n,n')^{113m,115m}\text{In}$ Measurements

These reactions are quite similar in most respects so they will be considered together.  $^{115}\text{In}$  is the majority isotope (95.72% abundance) and  $^{113}\text{In}$  is the minority isotope (4.28% abundance) [17]. For each isotope, the isomeric state has spin and parity  $\frac{1}{2}^-$  while the ground state is  $9/2^+$  [21]. The isomeric state in  $^{113}\text{In}$  has an excitation energy of 0.392 MeV and it decays 100% of the time to the ground state via an M4 transition with a half life of 99.4 m [21]. The isomeric state in  $^{115}\text{In}$  has an excitation energy of 0.335 MeV. It decays 94.5% of the time via an M4 transition to the ground state and 5.5% of the time via  $\beta^-$  emission to the stable ground state of  $^{115}\text{Sn}$ ; the decay half life is 4.5 h [21,23]. The electromagnetic transitions for both nuclei are internally converted quite strongly as can be seen from Table II. The 0.392-MeV gamma rays from  $^{113m}\text{In}$  and the 0.335-MeV gamma rays from  $^{115m}\text{In}$  were detected and their yields were utilized in determination of the reaction cross sections. No coincidence-summing corrections

were required.

### 3. EXPERIMENTAL RESULTS AND DISCUSSION

The results of our measurements are presented in both tabular (Tables V-VII) and graphical (Figs. 4-6) form in this report. The neutron energy and resolution are indicated in the first and second columns. The measured cross section ratio and experimental uncertainty appear in the third and fourth columns. Finally, the reaction cross section and its associated uncertainty, based on ENDF/B-IV values for the associated fission reactions [13], appear in the fifth and sixth columns. The cross section plots present the information in the first, second, fifth and sixth columns. Points from some data sets reported in the literature are joined by solid straight lines to provide a clearly visible representation of these data for comparison with our own results.

#### 3.1. $^{66}\text{Zn}(n,p)^{66}\text{Cu}$ Reaction

Our results for this reaction are shown in Table V and Fig. 4. No data was found in the literature for direct comparison with our own [24]. The cross section is small and has a relatively high effective threshold. Measurements near threshold were difficult because of the combined effects of short half life and low cross section. Some data has been reported for  $E_n \sim 14$  MeV [24] where the cross section appears to be  $\sim 70$  mb (which is consistent with our lower-energy data). The excitation curve for this reaction is reminiscent of that measured for the  $^{59}\text{Co}(n,p)^{59}\text{Fe}$  reaction [9] and it is suspected that the direct-reaction mechanism plays an important role in defining the shapes of these curves.

#### 3.2. $^{113,115}\text{In}(n,n')^{113m,115m}\text{In}$ Reactions

Our results for these reactions are shown in Tables VI and VII, and Figs. 5 and 6 respectively.

There is relatively little data available for the  $^{113}\text{In}(n,n')^{113\text{m}}\text{In}$  reaction. This process has been largely ignored because the abundance of  $^{113}\text{In}$  is only 4.28% while that of  $^{115}\text{In}$  is 95.72%. Our results are in good agreement with the values of Butler and Santry [25]. Agreement with the data of Grench and Menlove [26], near threshold, is fair and probably consistent with the experimental uncertainties. This reaction will probably never play a very important role in dosimetry applications because of low isotopic abundance.

The  $^{115}\text{In}(n,n')^{115\text{m}}\text{In}$  reaction is a popular dosimetry detector for several reasons. It has a low threshold, substantial cross section and the 0.335-MeV gamma ray is easily detected even though more than 50% of all decay transitions are internally converted. There are several cross section sets which can be compared with our data (Fig. 6) [25-31]. With the exception of the data of Martin et al. [31], in the region 4-5 MeV, all these data are in substantial agreement with our own. It appears that the  $^{115}\text{In}(n,n')^{115\text{m}}\text{In}$  reaction cross section is reasonably well known from threshold to  $\sim 10$  MeV.

#### 4. EYEGUIDES FOR EXPERIMENTAL DATA

The primary objective of our measurement program for neutron induced activation reactions is the provision of data for various applications. Our results generally approximate ideal monoenergetic cross sections because we have applied corrections for most effects which tend to integrate over neutron energy. However, our experimental data exhibit some redundancy and there are insignificant fluctuations which cannot be avoided in measured quantities. Therefore, we constructed eyeguide curves through our measured excitation functions which are based

on our subjective assessment of the significant information content. A sufficient number of points was selected from each curve to permit reconstruction of the curve by interpolation as discussed in earlier reports [9,10]. Tables VIII thru X contain the coordinates of these points for the  $^{66}\text{Zn}(n,p)^{66}\text{Cu}$ ,  $^{113}\text{In}(n,n')^{113\text{m}}\text{In}$  and  $^{115}\text{In}(n,n')^{115\text{m}}\text{In}$  reactions respectively. The eyeguide cross sections represented by these tables are based on ENDF/B-IV [13] values for the monitor fission reactions (Table I).

## 5. RESPONSE IN REFERENCE FISSION NEUTRON FIELDS

In an earlier report [10], we indicated the merits of testing monoenergetic cross section data in reference neutron fields. Two such fields, widely employed in reactor applications, are i) pure thermal-neutron fission of  $^{235}\text{U}$ , and, ii) spontaneous fission of  $^{252}\text{Cf}$ . Both these fields are quite well represented by simple mathematical formulas, of which the most commonly used is the Maxwellian distribution (Eq. (4) of Ref. 10). All details of the analysis and the corresponding nomenclature are presented in Ref. 10 and we follow the same procedure in the present work.

The results of our analysis are presented in Table XI and in Figs. 7-9. Our values of  $\bar{\sigma}$  for the  $^{66}\text{Zn}(n,p)^{66}\text{Cu}$  reaction are shown in parentheses since our data covers only part of the effective response range for this reaction (Fig. 7). We did not find any spectrum-averaged cross section values for this reaction reported in the literature [24].

Likewise, we did not find any spectrum-averaged cross section values for the  $^{113}\text{In}(n,n')^{113\text{m}}\text{In}$  reaction to compare with the results of our analysis [24]; such a comparison

would be meaningful since our data clearly covers essentially all of the response range of this reaction (Fig. 8).

There is an abundance of spectrum-averaged cross section values to compare with our value for the  $^{115}\text{In}(n,n')^{115\text{m}}\text{In}$  reaction [32-36]. We did not attempt a comprehensive survey of the literature, and selected only a few relatively recent values. This comparison is summarized in Table XII. Only the  $^{235}\text{U}$  thermal-neutron fission field was considered. There are sufficient differences in the origins of the values listed in Table XII to make quantitative comparison questionable. It is very gratifying, however, that a simple average of the values we selected from the literature is in excellent agreement ( $\sim 1\%$ ) with our value. All the values listed deviate from our value by no more than  $\sim 7\%$  which is within our experimental uncertainty (see Table IV).

## REFERENCES

1. "Compilation of Requests for Nuclear Data," USNDC-6 (LA-5233-MS), Los Alamos Scientific Laboratory (1974).
2. "WRENDA-74, World Request List for Nuclear Data Measurements-Fission Reactor Programmes," INDC (SEC)-38/U, International Atomic Energy Agency (1974).
3. "Request Lists of Nuclear Data for Controlled Fusion Research as Submitted to the International Atomic Energy Agency by Member States," INDC (NDS)-57/U+F, ed. J.R. Lemley, International Atomic Energy Agency (1973).
4. S. A. Cox and P. R. Hanley, IEE Trans. Nucl. Sci. 18, 108 (1971).
5. Donald L. Smith and James W. Meadows, Report No. ANL-7989, Argonne National Laboratory (1973).
6. D. L. Smith and J. W. Meadows, Trans. Amer. Nucl. Soc. 16, 312 (1973).
7. D. L. Smith and J. W. Meadows, Bull. Am. Phys. Soc. 19, 1031 (1974).
8. D. L. Smith and J. W. Meadows, Report No. ANL/NDM-9, Argonne National Laboratory (1974).
9. Donald L. Smith and James W. Meadows, Report No. ANL/NDM-10, Argonne National Laboratory (1975).
10. Donald L. Smith and James W. Meadows, Report No. ANL/NDM-13, Argonne National Laboratory (1975).
11. Donald G. Gardner, Bull. Am. Phys. Soc. 20, 162 (1975).
12. J. W. Meadows, Nucl. Sci. and Eng. 49, 310 (1972).
13. "Evaluated Nuclear Data File, ENDF/B-IV," National Neutron Cross Section Center, Brookhaven National Laboratory.
14. R. W. Lamphere, "Fission Detectors," in Fast Neutron Physics I, eds. J. B. Marion and J. L. Fowler, Interscience, New York, 721 (1960).
15. J. W. Meadows and D. L. Smith, Report No. ANL-7938, Argonne National Laboratory (1972).
16. J. M. Freeman and J. G. Jenkin, Nucl. Instr. Meth. 43, 269 (1966).
17. C. A. Rohrman, "Chart of the Nuclides," prepared at Battelle Pacific Northwest Laboratories under a contract to the U.S. Atomic Energy Commission (1969).
18. A. H. Wapstra and N. B. Gove, Nuclear Data Tables 9, 267 (1971).
19. M. J. Martin and M. N. Rao, Nuclear Data B2, 43 (1968).

20. R. S. Hager and E. G. Seltzer, Nuclear Data A4, 1 (1968).
21. "Nuclear Level Schemes A=45 through A=257," from Nuclear Data Sheets, ed. Nuclear Data Group, Oak Ridge National Laboratory, Academic Press, New York (1973).
22. H. Liskien and A. Paulsen, Nucl. Data 11, 569 (1973).
23. J. W. Rodgers, "LMFBR Reaction Rate and Dosimetry 5th Quarterly Progress Report," Report No. HEDL-TME-72-129 (Special Distribution), compiled by W. N. McElroy, Hanford Engineering Development Laboratory, p. ANC-24 (1972).
24. "CINDA-74: An Index to the Literature on Microscopic Neutron Data", International Atomic Energy Agency, Vienna (1974).
25. J. P. Butler and D. C. Santry, EANDC(Can)-34"L", p.3 (1968).
26. H. A. Grench and H. O. Menlove, Phys. Rev. 165, 1298 (1968).
27. H. O. Menlove, K. I. Coop and H. A. Grench, Phys. Rev. 163, 1308 (1967).
28. I. Kimura, K. Kobayashi and T. Shibata, Nucl. Sci. Tech. (Japan) 6, 485 (1971).
29. A. A. Ebel and C. Goodman, Phys. Rev. 93, 197 (1954).
30. K. Kobayashi, I. Kimura, H. Gotch and H. Yagi, Jour. Nucl. Energy 27, 741 (1973).
31. H. C. Martin, B. C. Diven and R. F. Taschek, Phys. Rev. 93, 199 (1954).
32. B. A. Magurno and O. Ozer, Nucl. Tech. 25, 376 (1975).
33. A. Fabry, Report BLG-465, Centre d'Etude de L'Energie Nucleaire, Mol, Belgium (1972).
34. A. Fabry, information communicated privately to A. B. Smith at a Specialist Meeting held at Harwell, U.K. (April 1975).
35. D. C. Santry and J. P. Butler, Bull. Am. Phys. Soc. 20, 171 (1975).
36. R. L. Simons and W. N. McElroy, Report BNWL-1312, Battelle Northwest Laboratories (1970).
37. J. Grundl and C. Eisenhauer, Bull. Am. Phys. Soc. 20, 145 (1975).
38. L. Cranberg, G. Frye, N. Nereson and L. Rosen, Phys. Rev. 103, 662 (1956).
39. W. N. McElroy and S. Berg, Report AFWL-TR-67-41, Vol III, Air Force Weapons Laboratory (1967).
40. B. E. Watt, Phys. Rev. 87, 1037 (1952).

Table I  
 ENDF/B-IV Fission Cross Sections<sup>a</sup>

A. <sup>235</sup>U(n,f) Cross Sections

$E_n$ (MeV)	$\sigma_F$ (barn)	$E_n$ (MeV)	$\sigma_F$ (barn)	$E_n$ (MeV)	$\sigma_F$ (barn)
0.1	1.585	1.4	1.25	6.7	1.445
0.15	1.458	1.6	1.258	7.0	1.549
0.2	1.351	1.8	1.267	7.5	1.682
0.25	1.308	2.0	1.274	8.0	1.758
0.3	1.28	2.5	1.275	9.0	1.804
0.4	1.216	3.0	1.232	10.0	1.768
0.5	1.172	4.0	1.15	11.0	1.718
0.6	1.152	5.0	1.094	12.0	1.767
0.7	1.135	5.5	1.059	13.0	1.976
0.8	1.133	5.75	1.075	14.0	2.152
0.9	1.174	6.0	1.16	15.0	2.23
1.0	1.225	6.2	1.232		
1.2	1.258	6.5	1.358		

B. <sup>238</sup>U(n,f) Cross Sections

$E_n$ (MeV)	$\sigma_F$ (barn)	$E_n$ (MeV)	$\sigma_F$ (barn)	$E_n$ (MeV)	$\sigma_F$ (barn)	$E_n$ (MeV)	$\sigma_F$ (barn)
0.1	$0.4 \times 10^{-4}$	1.2	0.0405	4.0	0.566	8.75	0.997
0.3	$0.7 \times 10^{-4}$	1.25	0.0426	4.5	0.563	9.0	0.992
0.5	$0.234 \times 10^{-3}$	1.3	0.0577	5.0	0.555	9.5	0.982
0.575	$0.566 \times 10^{-3}$	1.35	0.0933	5.2	0.560	10.0	0.974
0.61	0.00124	1.4	0.1512	5.4	0.563	11.0	0.983
0.7	0.00134	1.45	0.228	5.5	0.566	12.0	0.995
0.75	0.001985	1.5	0.294	5.8	0.603	13.0	1.048
9.8	0.003116	1.6	0.382	6.0	0.661	14.0	1.14
0.85	0.005871	1.7	0.437	6.2	0.723	15.0	1.26
0.89	0.008716	1.8	0.481	6.5	0.835	16.0	1.32
0.92	0.01278	1.9	0.514	6.8	0.897	17.0	1.34
0.95	0.0163	2.0	0.535	7.0	0.93	18.0	1.32
0.97	0.01609	2.1	0.545	7.2	0.957	19.0	1.3
1.0	0.01617	2.5	0.555	7.5	0.978	20.0	1.435
1.05	0.01812	2.75	0.55	8.0	0.99		
1.1	0.0235	3.0	0.542	8.25	0.996		
1.15	0.0349	3.5	0.555	8.5	1.0		

<sup>a</sup>Ref. 13.

Table II

Sample, Reaction and Decay  
Properties Required for Cross  
Section Determination

Sample Isotope	Abundance	Reaction Q-Value	Reaction Product	Decay Modes	Half Life	Gamma Ray Detected	Gamma Rays Per Disintegration	Total Internal Conversion
Zn -66	27.81% <sup>a</sup>	-1.852 MeV <sup>b</sup>	Cu-66	$\beta^-$ <sup>c</sup>	5.1 m <sup>c</sup>	1.039 MeV <sup>c</sup>	0.09 <sup>c</sup>	Negligible <sup>d</sup>
In-113	4.28% <sup>a</sup>	-0.392 MeV <sup>b</sup>	In-113M	$\gamma$ (IT) <sup>e</sup>	99.4 m <sup>e</sup>	0.392 MeV <sup>e</sup>	1.00 <sup>e</sup>	0.554 <sup>d</sup>
In-115	95.72% <sup>a</sup>	-0.335 MeV <sup>b</sup>	In-115M	$\gamma$ (IT) <sup>e</sup> , $\beta^-$	4.5 h <sup>e</sup>	0.335 MeV <sup>e</sup>	0.945 <sup>e</sup>	1.128 <sup>d</sup>

<sup>a</sup>Ref. 17.<sup>b</sup>Ref. 18.<sup>c</sup>Ref. 19.<sup>d</sup>Ref. 20.<sup>e</sup>Ref. 21.

## Table III

### Corrections Applied to Experimental Data

1. Geometry
2. Neutron Source-Properties
3. Decay Properties
4. Counting-Deadtime Losses
5. Sum Coincidences
6. Internal Conversion
7. Gamma-Ray Absorption
8. Neutron Absorption and Multiple Scattering
9. Fission-Detector Losses
10. Isotopic Abundances
11. Sample Impurities
12. Sample and Fission Deposit Masses

Table IV

Typical Values for Some Sources  
of Uncertainty in the Measured Cross Sections

Source of Uncertainty	Uncertainty
1. Counting statistics	Variable
2. Integration of gamma-ray full-energy peak	3%
3. Gamma-ray detector efficiency	5%
4. Decay half life	< 1%
5. Fission deposit and sample dimensions	1.4%
6. Neutron-group intensities	1-4%
7. Scattering corrections	1%
8. Mass of Uranium deposits	1%
9. Miscellaneous errors	1%

Table V

Experimental Results for the  
 $^{66}\text{Zn}(n,p)^{66}\text{Cu}$  Reaction

$^{238}\text{U}$  Monitor,  $\text{D}(d,n)^3\text{He}$  Neutron Source:

$E_n$ (MeV)	Resolution (MeV)	Measured $\sigma_{np}/\sigma_f$	Uncertainty in $\sigma_{np}/\sigma_f$	$\sigma_{np}^a$ (barn)	$\Delta\sigma_{np}^a$ (barn)
.5561E 01	.3690E 00	.1301E-01	.1809E-02	.7463E-02	.1038E-02
.6074E 01	.3718E 00	.1595E-01	.1493E-02	.1093E-01	.9615E-03
.6414E 01	.2986E 00	.1454E-01	.1367E-02	.1167E-01	.1098E-02
.6724E 01	.3000E 00	.1475E-01	.1239E-02	.1300E-01	.1092E-02
.7030E 01	.3032E 00	.1341E-01	.1543E-02	.1253E-01	.1441E-02
.7325E 01	.3076E 00	.1564E-01	.1361E-02	.1511E-01	.1314E-02
.7626E 01	.3130E 00	.1768E-01	.1592E-02	.1734E-01	.1561E-02
.7922E 01	.3192E 00	.1830E-01	.1721E-02	.1809E-01	.1700E-02
.7924E 01	.3192E 00	.1984E-01	.1488E-02	.1961E-01	.1470E-02
.8218E 01	.3260E 00	.2030E-01	.1624E-02	.2020E-01	.1616E-02
.8511E 01	.3334E 00	.2400E-01	.1848E-02	.2400E-01	.1848E-02
.8803E 01	.3412E 00	.2674E-01	.2127E-02	.2862E-01	.2119E-02
.9093E 01	.3494E 00	.2872E-01	.2756E-02	.2843E-01	.2729E-02
.9383E 01	.3580E 00	.3244E-01	.2465E-02	.3193E-01	.2426E-02
.9672E 01	.3668E 00	.3905E-01	.2421E-02	.3824E-01	.2371E-02
.9965E 01	.3762E 00	.3371E-01	.2460E-02	.3285E-01	.2396E-02

<sup>a</sup>Based on ENDF/B-IV fission cross sections (Table I and Ref. 13).

Table VI

Experimental Results for the  
 $^{113}\text{In}(n,n')^{113\text{m}}\text{In}$  (99.4m) Reaction

$^{235}\text{U}$  Monitor,  $^7\text{Li}(p,n)^7\text{Be}$  Neutron Source:

$E_n$ (MeV)	Resolution (MeV)	Measured $\sigma_{nn'}/\sigma_f$	Uncertainty in $\sigma_{nn'}/\sigma_f$	$\sigma_{nn'}^a$ (barn)	$\Delta\sigma_{nn'}^a$ (barn)
.7549E 00	.6862E-01	.1072E-01	.6109E-02	.1216E-01	.6927E-02
.9636E 00	.6860E-01	.1628E-01	.7157E-02	.1964E-01	.8634E-02
.1068E 01	.6880E-01	.2256E-01	.9704E-02	.2789E-01	.1200E-01
.1169E 01	.6920E-01	.5432E-01	.6578E-02	.6805E-01	.8241E-02
.1374E 01	.7000E-01	.8280E-01	.1069E-01	.1036E 00	.1338E-01
.1577E 01	.7114E-01	.1034E 00	.9066E-02	.1300E 00	.1140E-01
.1779E 01	.7250E-01	.1214E 00	.9495E-02	.1537E 00	.1202E-01
.1881E 01	.7324E-01	.1347E 00	.1051E-01	.1711E 00	.1335E-01
.1981E 01	.7402E-01	.1463E 00	.1143E-01	.1863E 00	.1455E-01
.2069E 01	.1006E 00	.1553E 00	.1024E-01	.1979E 00	.1305E-01
.2170E 01	.1008E 00	.1776E 00	.1155E-01	.2264E 00	.1472E-01
.2265E 01	.1012E 00	.2000E 00	.1267E-01	.2550E 00	.1615E-01
.2371E 01	.1016E 00	.2050E 00	.1290E-01	.2613E 00	.1644E-01
.2471E 01	.1020E 00	.2119E 00	.1353E-01	.2702E 00	.1726E-01
.2571E 01	.1026E 00	.2181E 00	.1394E-01	.2768E 00	.1769E-01
.2571E 01	.1026E 00	.2072E 00	.1305E-01	.2629E 00	.1656E-01
.2671E 01	.1032E 00	.2246E 00	.1395E-01	.2831E 00	.1758E-01
.2770E 01	.1036E 00	.2237E 00	.1390E-01	.2801E 00	.1740E-01
.2770E 01	.1036E 00	.2141E 00	.1326E-01	.2681E 00	.1660E-01
.2873E 01	.1044E 00	.2270E 00	.1427E-01	.2821E 00	.1773E-01
.2873E 01	.1044E 00	.2132E 00	.1301E-01	.2650E 00	.1617E-01
.2971E 01	.1050E 00	.2490E 00	.1545E-01	.3074E 00	.1908E-01
.2971E 01	.1050E 00	.2219E 00	.1356E-01	.2740E 00	.1674E-01

a

Based on ENDF/B-IV fission cross sections (Table I and Ref. 13).

Table VI (Contd.)

 $^{238}\text{U}$  Monitor,  $^7\text{Li}(p,n)^7\text{Be}$  Neutron Source:

$E_n$ (MeV)	Resolution (MeV)	Measured $\sigma_{nn'}/\sigma_f$	Uncertainty in $\sigma_{nn'}/\sigma_f$	$\sigma_{nn'}^a$ (barn)	$\Delta\sigma_{nn'}^a$ (barn)
.3169E 01	.1064E 00	.5451E 00	.3483E-01	.2979E 00	.1906E-01
.3369E 01	.1078E 00	.5043E 00	.3026E-01	.2782E 00	.1669E-01
.3568E 01	.1094E 00	.5049E 00	.3085E-01	.2810E 00	.1717E-01
.3769E 01	.1112E 00	.4920E 00	.2993E-01	.2759E 00	.1679E-01
.4365E 01	.1176E 00	.4496E 00	.2741E-01	.2535E 00	.1545E-01
.4563E 01	.1196E 00	.4450E 00	.2755E-01	.2501E 00	.1548E-01
.4759E 01	.1206E 00	.4670E 00	.2894E-01	.2610E 00	.1617E-01
.4941E 01	.1586E 00	.5181E 00	.3315E-01	.2880E 00	.1843E-01
.5141E 01	.1598E 00	.4735E 00	.3032E-01	.2645E 00	.1693E-01
.5338E 01	.1612E 00	.5090E 00	.3104E-01	.2861E 00	.1745E-01
.5534E 01	.1626E 00	.5231E 00	.3192E-01	.2983E 00	.1820E-01
.5734E 01	.1642E 00	.5416E 00	.3355E-01	.3222E 00	.1996E-01
.5750E 01	.1312E 00	.5654E 00	.3837E-01	.3374E 00	.2290E-01

 $^{238}\text{U}$  Monitor,  $\text{D}(d,n)^3\text{He}$  Neutron Source:

$E_n$ (MeV)	Resolution (MeV)	Measured $\sigma_{nn'}/\sigma_f$	Uncertainty in $\sigma_{nn'}/\sigma_f$	$\sigma_{nn'}^a$ (barn)	$\Delta\sigma_{nn'}^a$ (barn)
.5064E 01	.3294E 00	.5296E 00	.3287E-01	.2948E 00	.1829E-01
.5425E 01	.3124E 00	.5224E 00	.3192E-01	.2945E 00	.1800E-01
.5756E 01	.3034E 00	.5003E 00	.3198E-01	.2989E 00	.1911E-01
.6406E 01	.2984E 00	.3614E 00	.2209E-01	.2891E 00	.1767E-01
.6721E 01	.2998E 00	.2844E 00	.1818E-01	.2505E 00	.1601E-01
.7034E 01	.3030E 00	.2578E 00	.1651E-01	.2409E 00	.1543E-01
.7330E 01	.3072E 00	.2542E 00	.1577E-01	.2456E 00	.1524E-01
.7640E 01	.3130E 00	.2629E 00	.1600E-01	.2581E 00	.1570E-01
.7957E 01	.3194E 00	.2591E 00	.1579E-01	.2562E 00	.1561E-01
.8250E 01	.3266E 00	.2493E 00	.1518E-01	.2484E 00	.1512E-01
.8533E 01	.3336E 00	.2441E 00	.1491E-01	.2440E 00	.1490E-01
.8843E 01	.3418E 00	.2350E 00	.1456E-01	.2339E 00	.1449E-01
.9146E 01	.3506E 00	.2309E 00	.1407E-01	.2284E 00	.1391E-01
.9429E 01	.3590E 00	.2085E 00	.1270E-01	.2051E 00	.1249E-01
.9740E 01	.3686E 00	.2216E 00	.1352E-01	.2167E 00	.1322E-01
1.0035E 02	.3778E 00	.2122E 00	.1296E-01	.2068E 00	.1262E-01

<sup>a</sup>Based on ENDF/B-IV fission cross sections (Table I and Ref. 13).

Table VII

Experimental Results for the  
 $^{115}\text{In}(n,n')^{115\text{m}}\text{In}$  (4.5 h) Reaction

$^{235}\text{U}$  Monitor,  $^7\text{Li}(p,n)^7\text{Be}$  Neutron Source:

$E_n$ (MeV)	Resolution (MeV)	Measured $\sigma_{nn'}/\sigma_f$	Uncertainty in $\sigma_{nn'}/\sigma_f$	$\sigma_{nn'}^a$ (barn)	$\Delta\sigma_{nn'}^a$ (barn)
.4437E 00	.4568E-01	.1617E-02	.8584E-03	.1935E-02	.1027E-02
.4490E 00	.4574E-01	.1955E-02	.5864E-03	.2291E-02	.6873E-03
.5528E 00	.4588E-01	.2624E-02	.5351E-03	.3047E-02	.6215E-03
.6072E 00	.4600E-01	.5030E-02	.7398E-03	.5789E-02	.8513E-03
.6495E 00	.6898E-01	.1093E-01	.9751E-03	.1249E-01	.1115E-02
.7549E 00	.6862E-01	.1758E-01	.1617E-02	.1993E-01	.1834E-02
.9634E 00	.6860E-01	.5096E-01	.3354E-02	.6147E-01	.4046E-02
.1168E 01	.6910E-01	.9120E-01	.5569E-02	.1142E 00	.6976E-02
.1374E 01	.7000E-01	.1210E 00	.7637E-02	.1514E 00	.9554E-02
.1577E 01	.7114E-01	.1431E 00	.8748E-02	.1799E 00	.1100E-01
.1779E 01	.7250E-01	.1743E 00	.1066E-01	.2207E 00	.1350E-01
.1881E 01	.7324E-01	.1871E 00	.1132E-01	.2376E 00	.1437E-01
.1981E 01	.7402E-01	.2095E 00	.1280E-01	.2668E 00	.1630E-01
.2069E 01	.1006E 00	.2078E 00	.1248E-01	.2648E 00	.1591E-01
.2169E 01	.1008E 00	.2440E 00	.1464E-01	.3109E 00	.1865E-01
.2265E 01	.1012E 00	.2527E 00	.1516E-01	.3221E 00	.1932E-01
.2371E 01	.1016E 00	.2634E 00	.1582E-01	.3357E 00	.2016E-01
.2471E 01	.1020E 00	.2645E 00	.1585E-01	.3372E 00	.2021E-01
.2571E 01	.1026E 00	.2719E 00	.1679E-01	.3450E 00	.2130E-01
.2571E 01	.1026E 00	.2586E 00	.1550E-01	.3282E 00	.1967E-01
.2671E 01	.1032E 00	.2822E 00	.1695E-01	.3556E 00	.2136E-01
.2770E 01	.1036E 00	.2916E 00	.1750E-01	.3651E 00	.2190E-01
.2770E 01	.1036E 00	.2741E 00	.1646E-01	.3431E 00	.2060E-01
.2873E 01	.1044E 00	.2764E 00	.1658E-01	.3436E 00	.2060E-01
.2873E 01	.1044E 00	.2699E 00	.1618E-01	.3355E 00	.2011E-01
.2971E 01	.1050E 00	.2959E 00	.1775E-01	.3653E 00	.2192E-01
.2971E 01	.1050E 00	.2737E 00	.1641E-01	.3379E 00	.2025E-01

<sup>a</sup>

Based on ENDF/B-IV fission cross sections (Table I and Ref. 13).

Table VII (Contd.)

$^{238}\text{U}$  Monitor,  $^7\text{Li}(p,n)^7\text{Be}$  Neutron Source:

$E_n$ (MeV)	Resolution (MeV)	Measured $\sigma_{nn'}/\sigma_f$	Uncertainty in $\sigma_{nn'}/\sigma_f$	$\sigma_{nn'}^a$ (barn)	$\Delta\sigma_{nn'}^a$ (barn)
.3369E 01	.1078E 00	.6199E 00	.3716E-01	.3420E 00	.2050E-01
.3568E 01	.1094E 00	.6190E 00	.3712E-01	.3445E 00	.2066E-01
.3769E 01	.1112E 00	.6079E 00	.3648E-01	.3410E 00	.2046E-01
.4365E 01	.1165E 00	.5676E 00	.3409E-01	.3200E 00	.1922E-01
.4563E 01	.1185E 00	.5734E 00	.3438E-01	.3222E 00	.1932E-01
.4759E 01	.1205E 00	.5814E 00	.3488E-01	.3249E 00	.1950E-01
.4941E 01	.1586E 00	.6401E 00	.3841E-01	.3559E 00	.2135E-01
.5140E 01	.1598E 00	.5783E 00	.3470E-01	.3230E 00	.1938E-01
.5338E 01	.1612E 00	.6097E 00	.3640E-01	.3427E 00	.2046E-01
.5534E 01	.1626E 00	.6082E 00	.3653E-01	.3468E 00	.2083E-01
.5733E 01	.1642E 00	.6030E 00	.3611E-01	.3586E 00	.2148E-01
.5750E 01	.1312E 00	.5874E 00	.3531E-01	.3506E 00	.2108E-01

$^{238}\text{U}$  Monitor,  $\text{D}(d,n)^3\text{He}$  Neutron Source:

$E_n$ (MeV)	Resolution (MeV)	Measured $\sigma_{nn'}/\sigma_f$	Uncertainty in $\sigma_{nn'}/\sigma_f$	$\sigma_{nn'}^a$ (barn)	$\Delta\sigma_{nn'}^a$ (barn)
.5063E 01	.3294E 00	.6433E 00	.3869E-01	.3580E 00	.2153E-01
.5423E 01	.3124E 00	.6424E 00	.3847E-01	.3621E 00	.2168E-01
.5755E 01	.3034E 00	.6191E 00	.3714E-01	.3699E 00	.2219E-01
.6406E 01	.2984E 00	.4524E 00	.2717E-01	.3619E 00	.2173E-01
.6721E 01	.2998E 00	.3665E 00	.2195E-01	.3227E 00	.1933E-01
.7035E 01	.3030E 00	.3376E 00	.2024E-01	.3156E 00	.1891E-01
.7330E 01	.3072E 00	.3180E 00	.1909E-01	.3073E 00	.1845E-01
.7647E 01	.3130E 00	.3302E 00	.1977E-01	.3241E 00	.1941E-01
.7957E 01	.3194E 00	.3084E 00	.1852E-01	.3050E 00	.1832E-01
.8256E 01	.3266E 00	.3052E 00	.1830E-01	.3040E 00	.1823E-01
.8553E 01	.3336E 00	.3021E 00	.1811E-01	.3020E 00	.1810E-01
.8843E 01	.3418E 00	.2908E 00	.1748E-01	.2894E 00	.1739E-01
.9146E 01	.3506E 00	.2743E 00	.1644E-01	.2713E 00	.1626E-01
.9430E 01	.3590E 00	.2612E 00	.1569E-01	.2568E 00	.1543E-01
.9741E 01	.3686E 00	.2643E 00	.1586E-01	.2585E 00	.1551E-01
.1003E 02	.3778E 00	.2449E 00	.1469E-01	.2386E 00	.1431E-01

<sup>a</sup> Based on ENDF/B-IV fission cross sections (Table I and Ref. 13).

Table VIII

 $^{66}\text{Zn}(n,p)^{66}\text{Cu}$  Reaction Eyeguide Cross Sections<sup>a</sup>

$E_n$ (MeV)	$\sigma_{np}$ (barn)
.5500E 01	.7477E-02
.6000E 01	.9948E-02
.6500E 01	.1203E-01
.7000E 01	.1332E-01
.7250E 01	.1466E-01
.7500E 01	.1600E-01
.7750E 01	.1751E-01
.8000E 01	.1922E-01
.8250E 01	.2114E-01
.8500E 01	.2330E-01
.8750E 01	.2560E-01
.9000E 01	.2805E-01
.9250E 01	.3060E-01
.9500E 01	.3303E-01
.9750E 01	.3530E-01
.1000E 02	.3745E-01

<sup>a</sup>

Based on  $\sigma_{np}/\sigma_f$  ratios measured in present work (Table V) and ENDF/B-IV fission cross sections [13].

Table IX

$^{113}\text{In}(n,n')^{113\text{m}}\text{In}$  (99.4 m) Reaction  
 Eyeguide Cross Sections<sup>a</sup>

$E_n$ (MeV)	$\sigma_{nn'}$ (barn)	$E_n$ (MeV)	$\sigma_{nn'}$ (barn)
.7500E 00	.1145E-01	.4000E 01	.2651E 00
.9000E 00	.1686E-01	.4300E 01	.2547E 00
.1000E 01	.2281E-01	.4400E 01	.2523E 00
.1050E 01	.2644E-01	.4600E 01	.2515E 00
.1100E 01	.3512E-01	.4700E 01	.2540E 00
.1150E 01	.5953E-01	.4900E 01	.2653E 00
.1200E 01	.7509E-01	.5100E 01	.2824E 00
.1300E 01	.9187E-01	.5200E 01	.2893E 00
.1400E 01	.1075E 00	.5400E 01	.2977E 00
.1500E 01	.1207E 00	.5600E 01	.3015E 00
.1700E 01	.1452E 00	.5800E 01	.3021E 00
.1800E 01	.1565E 00	.6000E 01	.3113E 00
.1900E 01	.1728E 00	.6200E 01	.2959E 00
.2000E 01	.1889E 00	.6400E 01	.2837E 00
.2050E 01	.1944E 00	.6600E 01	.2623E 00
.2100E 01	.2029E 00	.6700E 01	.2523E 00
.2200E 01	.2313E 00	.6800E 01	.2447E 00
.2250E 01	.2432E 00	.7000E 01	.2374E 00
.2300E 01	.2531E 00	.7300E 01	.2437E 00
.2400E 01	.2629E 00	.7500E 01	.2490E 00
.2500E 01	.2677E 00	.7600E 01	.2530E 00
.2600E 01	.2719E 00	.7800E 01	.2562E 00
.2800E 01	.2787E 00	.8000E 01	.2542E 00
.3000E 01	.2845E 00	.8500E 01	.2420E 00
.3200E 01	.2879E 00	.9000E 01	.2306E 00
.3400E 01	.2832E 00	.1000E 02	.2046E 00
.3600E 01	.2690E 00		

a

Based on  $\sigma_{nn'}/\sigma_f$  ratios measured in present work (Table VI) and ENDF/B-IV fission cross sections [13].

Table X

 $^{115}\text{In}(n,n')^{115\text{m}}\text{In}$  (4.5 h) Reaction  
 Eyeguide Cross Sections<sup>a</sup>

$E_n$ (MeV)	$\sigma_{nn'}$ (barn)	$E_n$ (MeV)	$\sigma_{nn'}$ (barn)
.4600E 00	.1994E-02	.2600E 01	.3381E 00
.5000E 00	.2261E-02	.2700E 01	.3414E 00
.5400E 00	.2739E-02	.2800E 01	.3438E 00
.5600E 00	.3185E-02	.2900E 01	.3453E 00
.5800E 00	.3900E-02	.3000E 01	.3480E 00
.6000E 00	.5192E-02	.3200E 01	.3495E 00
.6200E 00	.7878E-02	.3500E 01	.3410E 00
.6300E 00	.9968E-02	.3900E 01	.3314E 00
.6400E 00	.1136E-01	.4200E 01	.3249E 00
.6600E 00	.1323E-01	.4400E 01	.3210E 00
.6800E 00	.1481E-01	.4600E 01	.3188E 00
.7200E 00	.1739E-01	.4700E 01	.3180E 00
.7600E 00	.2044E-01	.4800E 01	.3193E 00
.8000E 00	.2460E-01	.4900E 01	.3228E 00
.8400E 00	.3007E-01	.5000E 01	.3272E 00
.8800E 00	.3715E-01	.5100E 01	.3378E 00
.9200E 00	.4746E-01	.5200E 01	.3478E 00
.9400E 00	.5345E-01	.5300E 01	.3550E 00
.9600E 00	.6016E-01	.5400E 01	.3552E 00
.1000E 01	.7241E-01	.5500E 01	.3527E 00
.1040E 01	.8321E-01	.5700E 01	.3555E 00
.1100E 01	.9833E-01	.5800E 01	.3558E 00
.1160E 01	.1134E 00	.5900E 01	.3637E 00
.1200E 01	.1218E 00	.6000E 01	.3701E 00
.1260E 01	.1325E 00	.6200E 01	.3596E 00
.1300E 01	.1403E 00	.6400E 01	.3532E 00
.1360E 01	.1499E 00	.6600E 01	.3418E 00
.1440E 01	.1628E 00	.6800E 01	.3260E 00
.1500E 01	.1739E 00	.7000E 01	.3110E 00
.1600E 01	.1896E 00	.7300E 01	.3109E 00
.1700E 01	.2052E 00	.7600E 01	.3052E 00
.1800E 01	.2213E 00	.8200E 01	.3034E 00
.1900E 01	.2372E 00	.8400E 01	.3012E 00
.2000E 01	.2616E 00	.8600E 01	.2970E 00
.2100E 01	.2863E 00	.8800E 01	.2899E 00
.2150E 01	.3011E 00	.9000E 01	.2795E 00
.2200E 01	.3130E 00	.9200E 01	.2692E 00
.2250E 01	.3191E 00	.9400E 01	.2618E 00
.2300E 01	.3232E 00	.9600E 01	.2536E 00
.2400E 01	.3295E 00	.9800E 01	.2435E 00
.2500E 01	.3360E 00	.1000E 02	.2454E 00

<sup>a</sup>Based on  $\sigma_{nn'}/\sigma_f$  ratios measured in present work (Table VII) and ENDF/B-IV fission cross sections [13].

Table XI

## Summary of Response Calculation Results

Reaction "j"	E <sub>min</sub> (MeV)	E <sub>max</sub> (MeV)	$\bar{\sigma}_j (E_{av}, E_{min}, E_{max}), \text{mb}^a$	
			E <sub>av</sub> = 1.97 MeV	E <sub>av</sub> = 2.13 MeV
$^{66}\text{Zn}(n,p)^{66}\text{Cu}$	5.5	10.0	(0.501)	(0.675)
$^{113}\text{In}(n,n')^{113\text{m}}\text{In}$ (99.4 m)	0.75	10.0	134	143
$^{115}\text{In}(n,n')^{115\text{m}}\text{In}$ (4.5 h)	0.46	10.0	179	189

<sup>a</sup> $\bar{\sigma}_j (E_{av}, E_{min}, E_{max})$  computed using the Maxwellian distribution (Eq. (4) from Ref. 10).  $E_{av} = 1.97$  MeV corresponds to the neutron field from pure thermal fission of  $^{235}\text{U}$  while  $E_{av} = 2.13$  MeV corresponds to the spontaneous fission neutron field from  $^{252}\text{Cf}$  [37]. Values shown in parentheses correspond to cases where our experimental data fail to cover a significant portion of the response range (see Figs. 7-9).

Table XII

Comparison of Response Calculation Results  
for the  $^{115}\text{In}(n,n')^{115\text{m}}\text{In}$  Reaction in a  
 $^{235}\text{U}$  Thermal Fission Neutron Field with  
Some Similar Values from the Literature

Source	$\bar{\sigma}_f$ ( $X_{25}$ , $^{115}\text{In}$ ), mb
1. Present work (1975)	179
2. ENDF/B-IV Dosimetry File (1975). <sup>a</sup>	166.8
3. Fabry: Evaluation of Integral Data (1972). <sup>b</sup>	188 ± 4
4. Fabry: Response of ENDF/B-IV monoenergetic cross sections in NBS (USA) Evaluated spectrum (1975). <sup>c</sup>	181.3 <i>Should be 167 mb. 9/8/75.</i>
5. Santry and Butler: Response of their measured monoenergetic data in spectrum from Cranberg et al. <sup>d</sup>	173 ± 9
6. Simons and McElroy: Response of 1967 SAND-II cross section set in the Watt Spectrum. <sup>e</sup>	174
Simple average of literature values (Nos.2-6)	177

<sup>a</sup> Refs. 13 and 32.

<sup>b</sup> Ref. 33.

<sup>c</sup> Refs. 13, 34 and 37.

<sup>d</sup> Refs. 35 and 38.

<sup>e</sup> Refs. 36, 39, 40.

## FIGURE CAPTIONS

- Fig. 1. Sample irradiation apparatus used for the present set of measurements. The gas target assembly shown was employed for irradiations with neutrons from the  $D(d,n)^3\text{He}$  reaction. The lithium target assembly used for lower-energy irradiations is not shown. (ANL Neg. No. 116-2355 Rev. 1)
- Fig. 2. Ge(Li) detector sample counting apparatus used for  $^{113}\text{In}$  and  $^{115}\text{In}$  measurements. The NaI(Tl) scintillation detector used for the  $^{66}\text{Zn}$  measurements is not shown. (ANL Neg.No.116-2531)
- Fig. 3. Schematic representation of the multiple-scattering corrections applied to the experimental data. (ANL Neg. No. 116-1174)
- Fig. 4. Cross sections for the  $^{66}\text{Zn}(n,p)^{66}\text{Cu}$  reaction based on measured  $\sigma_{np}/\sigma_f$  cross section ratios and ENDF/B-IV fission cross sections. (ANL Neg. No. 116-2721)
- Fig. 5. Cross sections for the  $^{113}\text{In}(n,n')^{113m}\text{In}$  (99.4 m) reaction based on measured  $\sigma_{nn'}/\sigma_f$  cross section ratios and ENDF/B-IV fission cross sections. Other selected values from the literature are indicated by labelled solid curves. (ANL Neg. No. 116-2719)
- Fig. 6. Cross sections for the  $^{115}\text{In}(n,n')^{115m}\text{In}$  (4.5 h) reaction based on measured  $\sigma_{nn'}/\sigma_f$  cross section ratios and ENDF/B-IV fission cross sections. Other selected values from the literature are indicated by labelled solid curves (ANL Neg. No. 116-2720).
- Figs.7 thru 9. Response of the  $^{66}\text{Zn}(n,p)^{66}\text{Cu}$ ,  $^{113}\text{In}(n,n')^{113m}\text{In}$  and  $^{115}\text{In}(n,n')^{115m}\text{In}$  reactions in reference neutron fields corresponding to i) thermal-neutron fission of  $^{235}\text{U}$ , and ii) spontaneous fission of  $^{252}\text{Cf}$ . Symbols: (+) Points representing eyeguide,  $\sigma(E)$ , to the experimental data. Dashed line shows the reference neutron spectrum,  $X(E)$ . Solid line shows the response function,  $R(E) = X(E) \cdot \sigma(E)$ . Plots are arbitrarily normalized to place maxima for each curve at the top border of the frame. (ANL Neg. Nos. 116-2761,-2763,-2762 respectively)

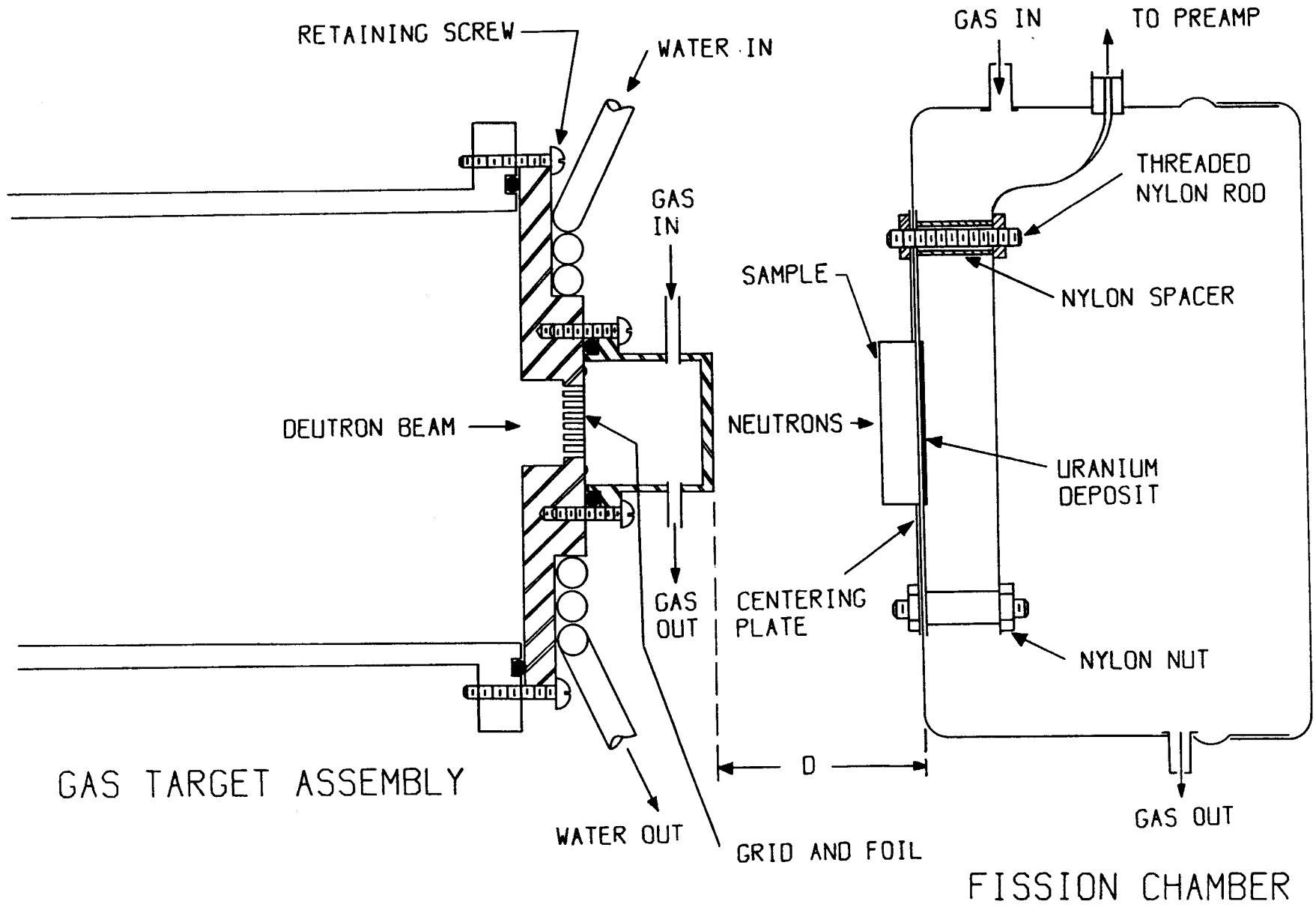


Fig. 1

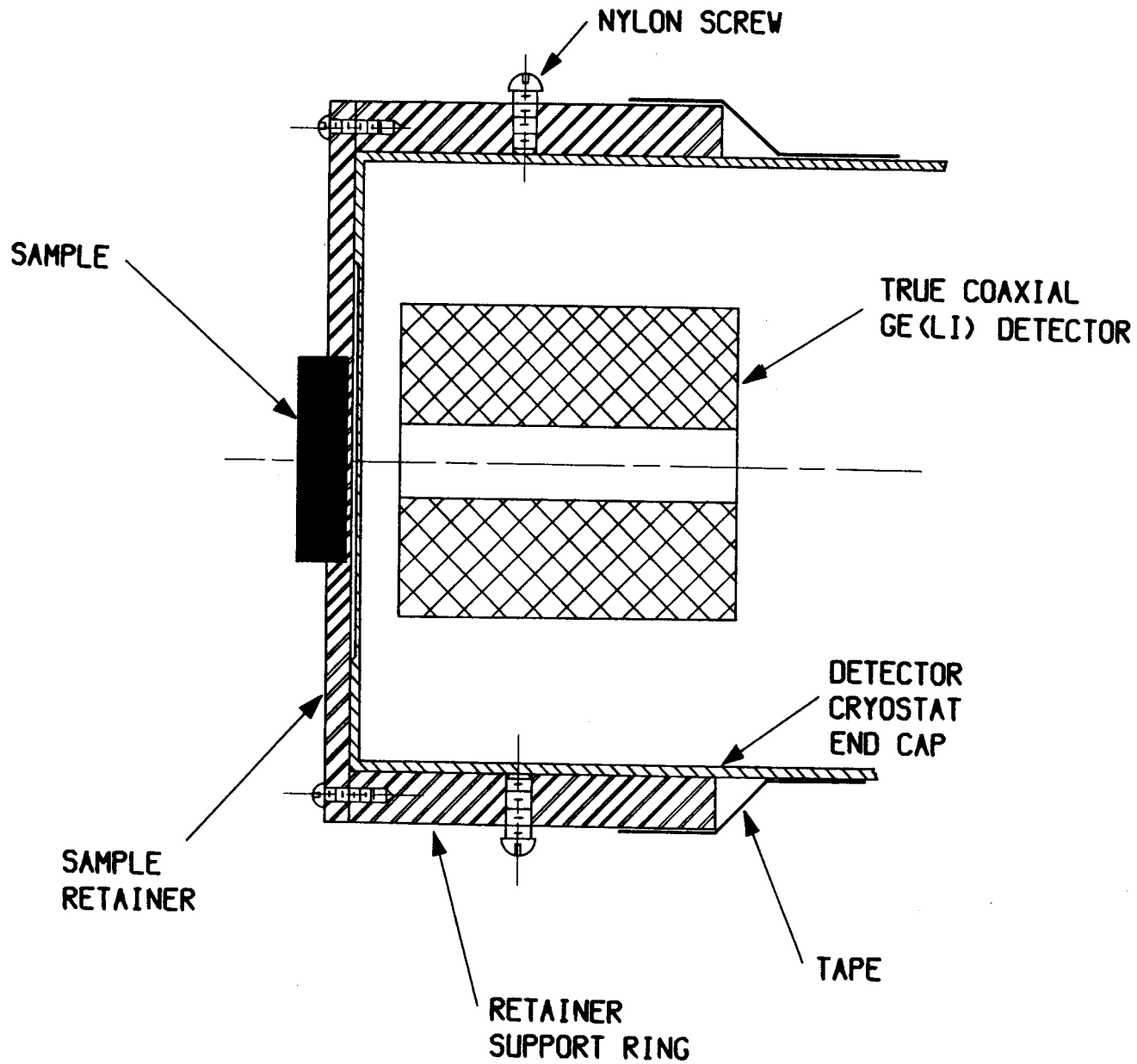
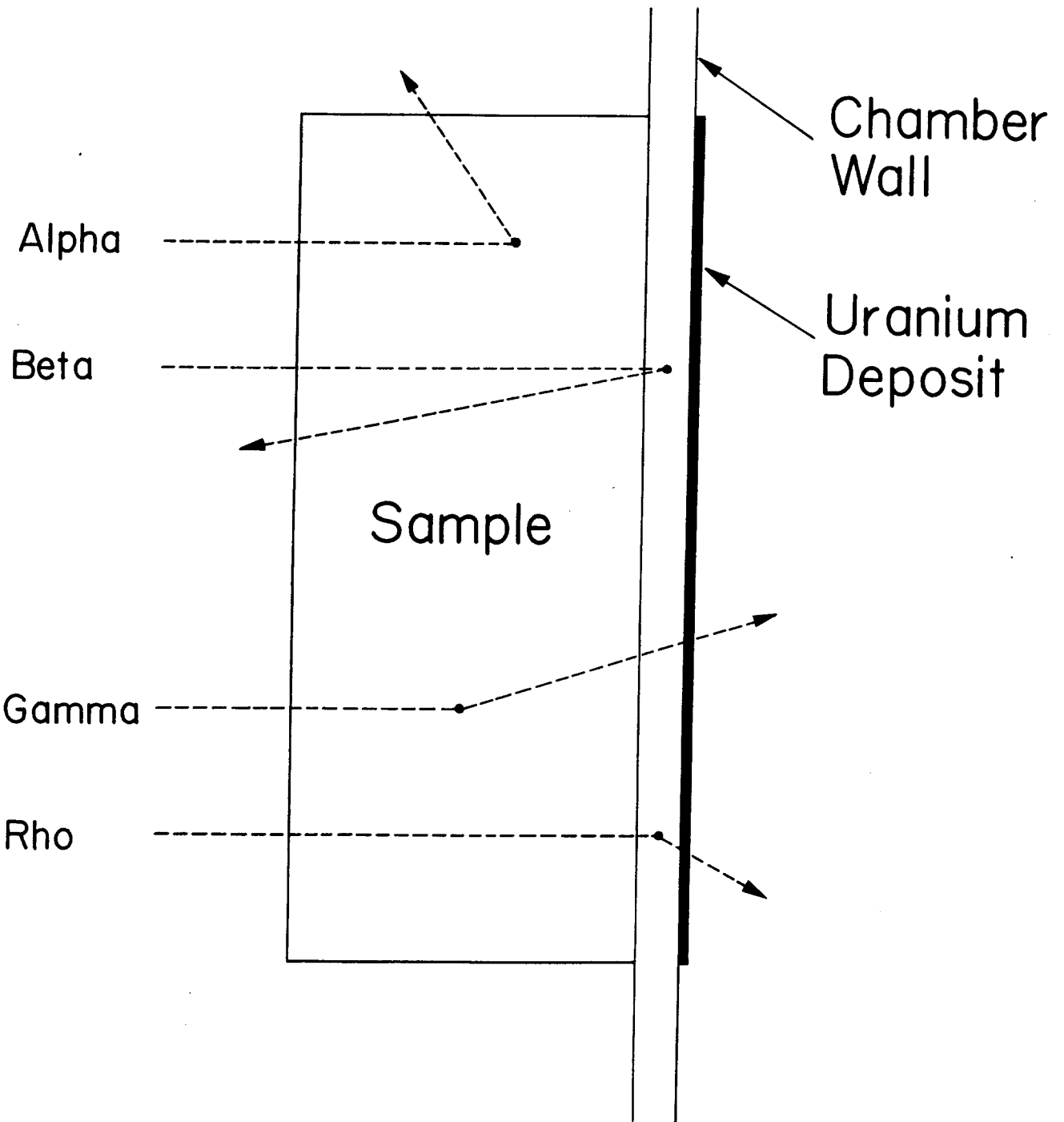


Fig. 2

Fig. 3



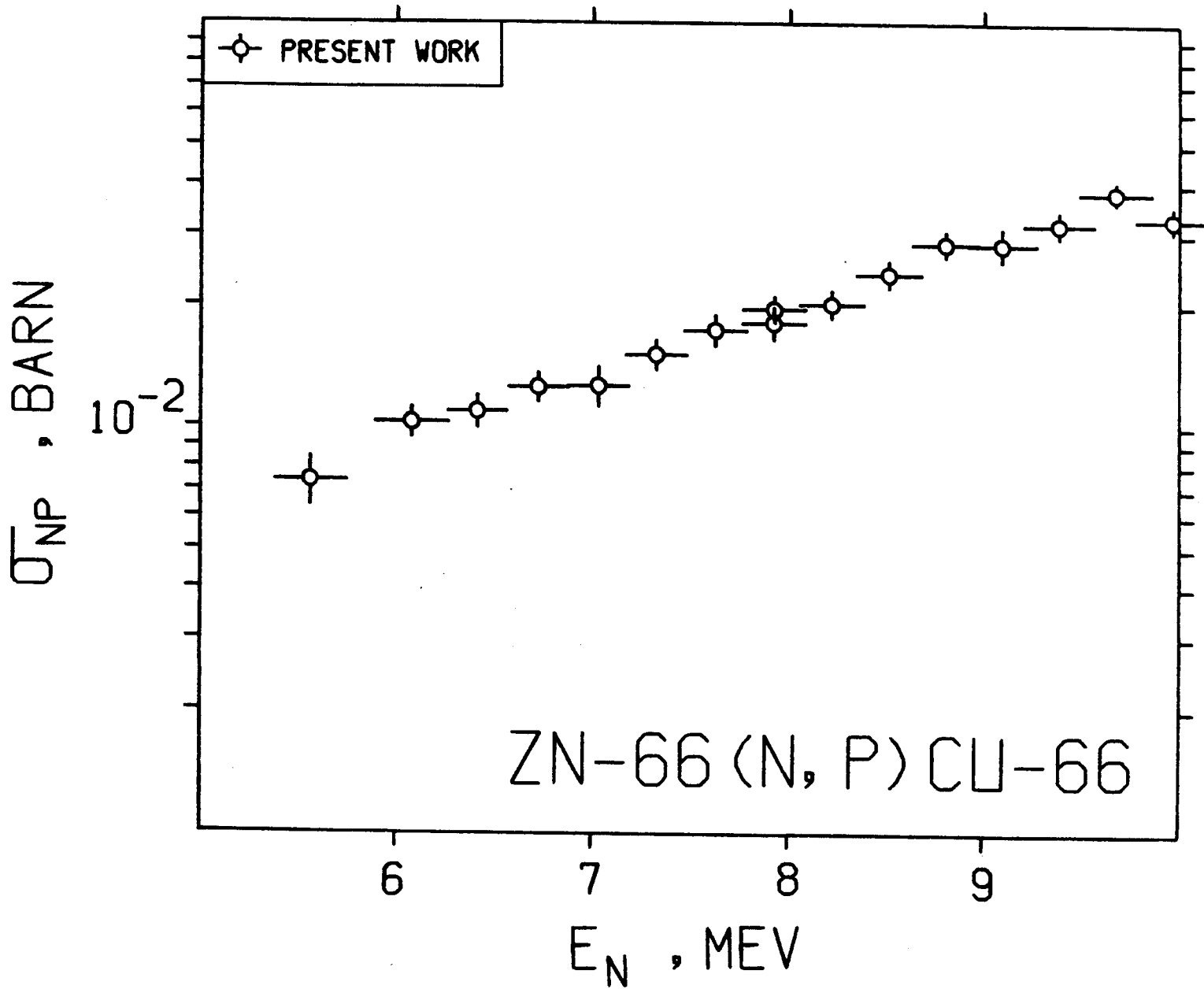


FIG. 4

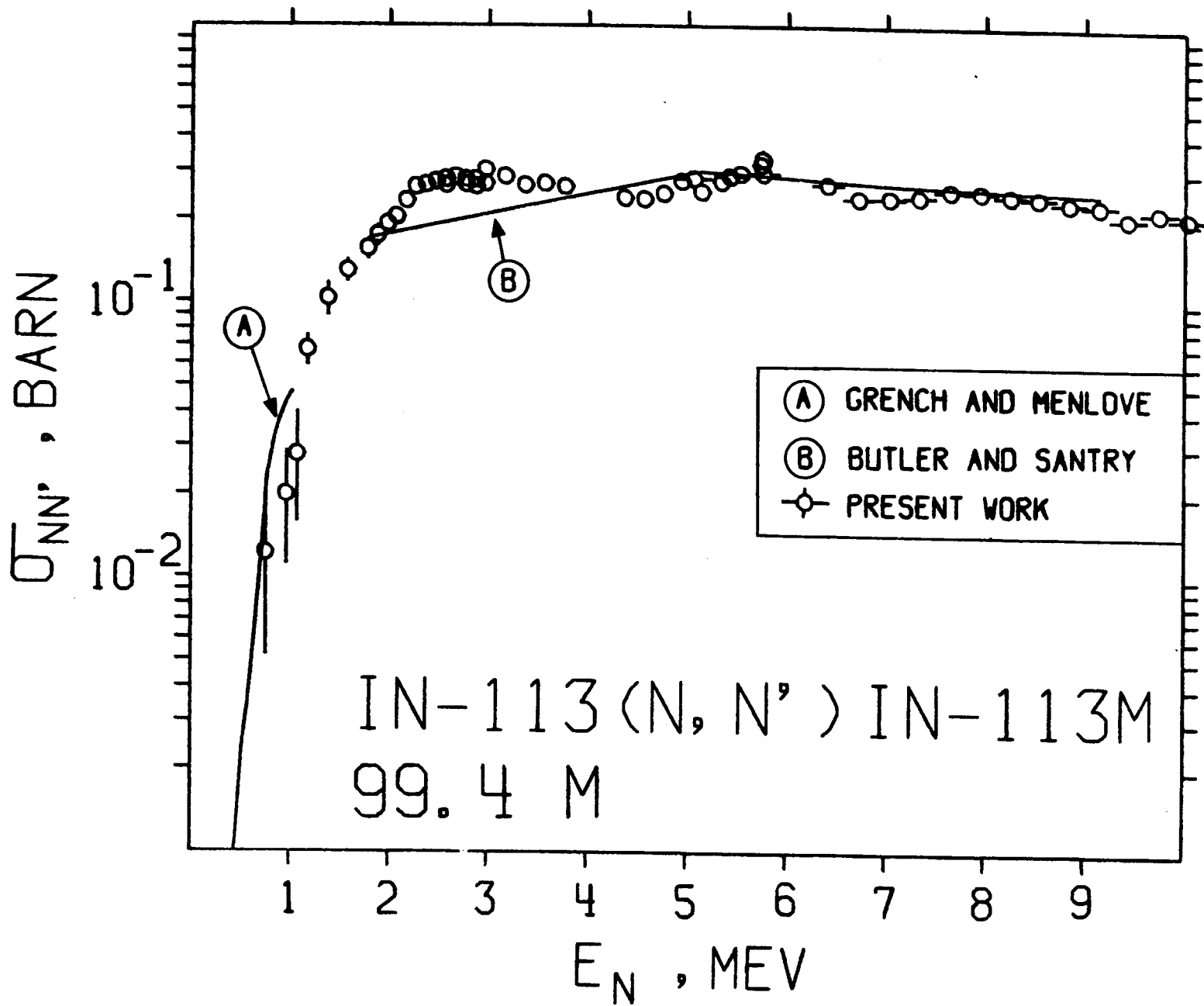


FIG. 5

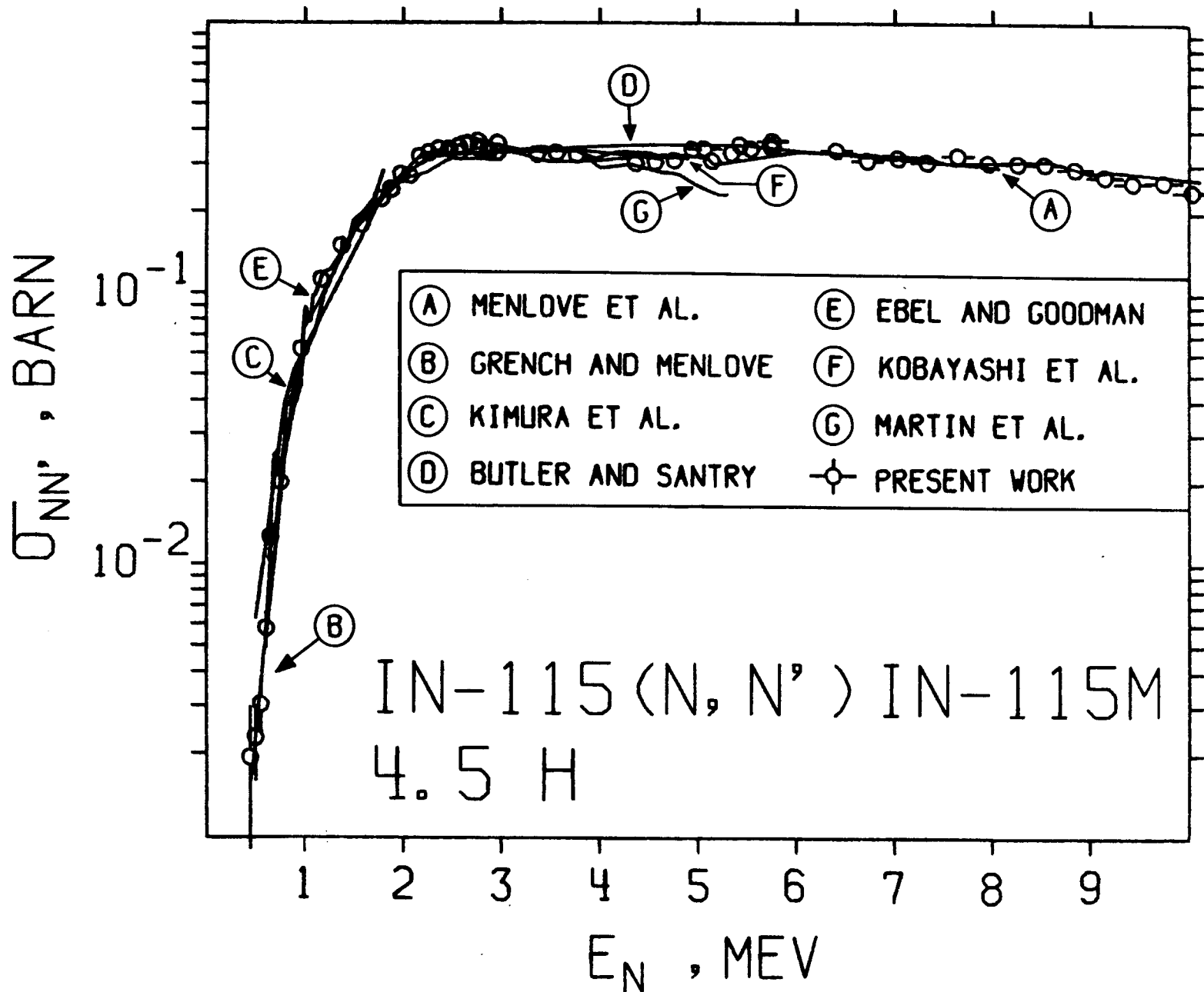


Fig. 6

Fig. 7

# ZN-66 (N, P) CU-66

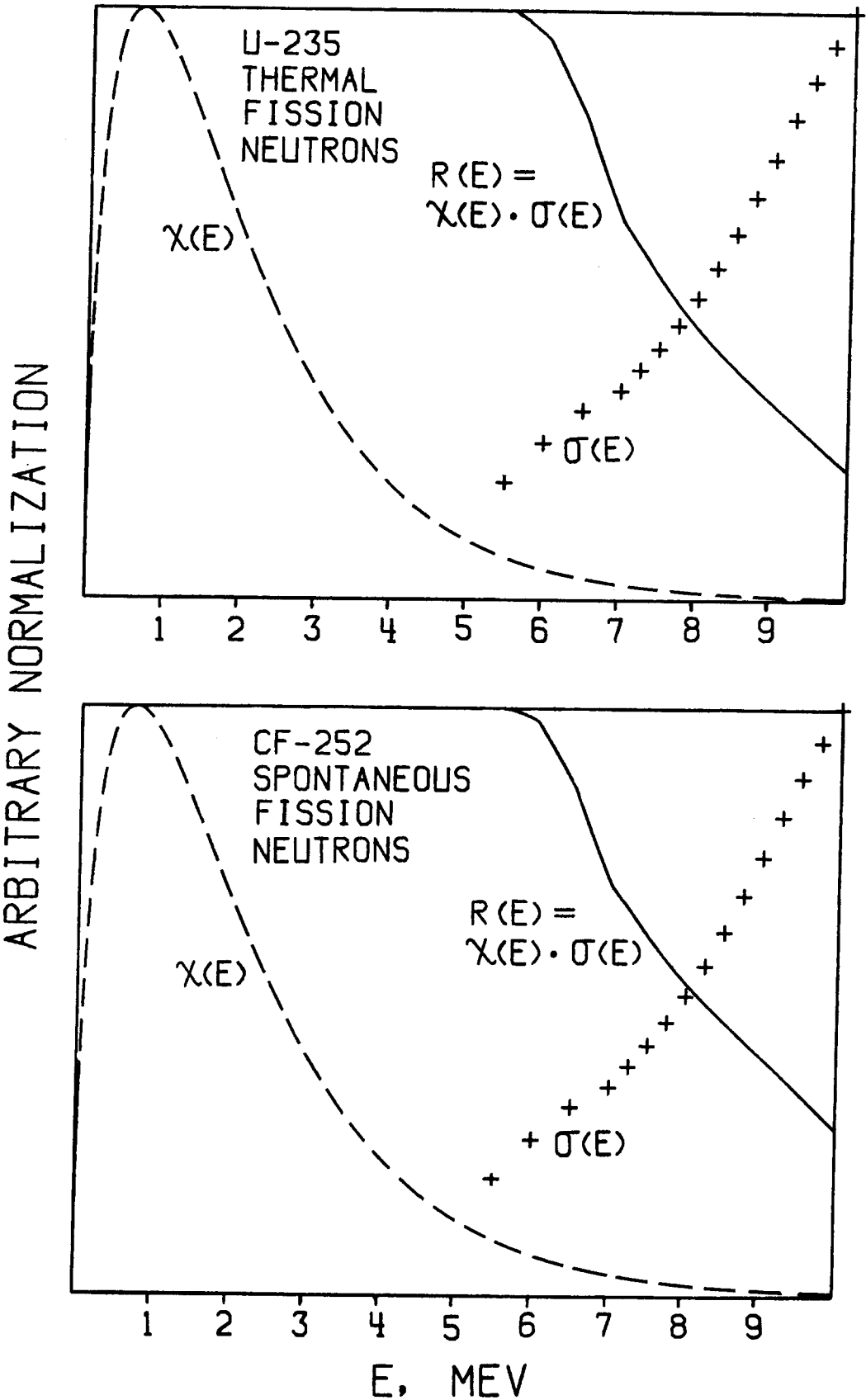
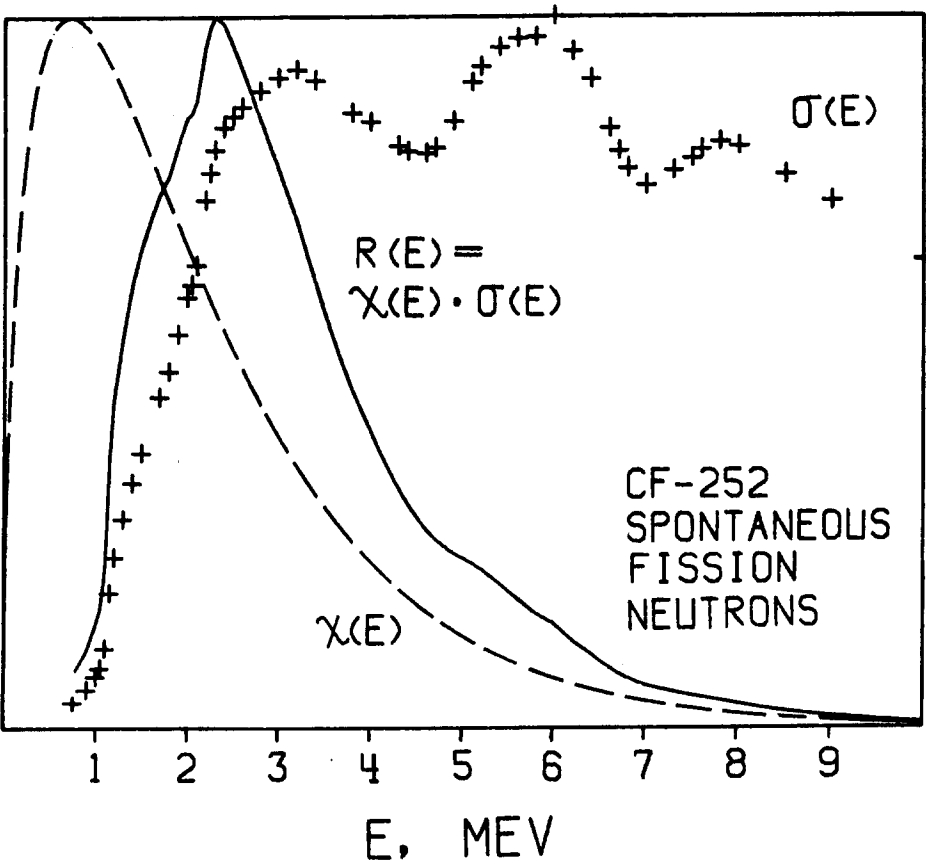
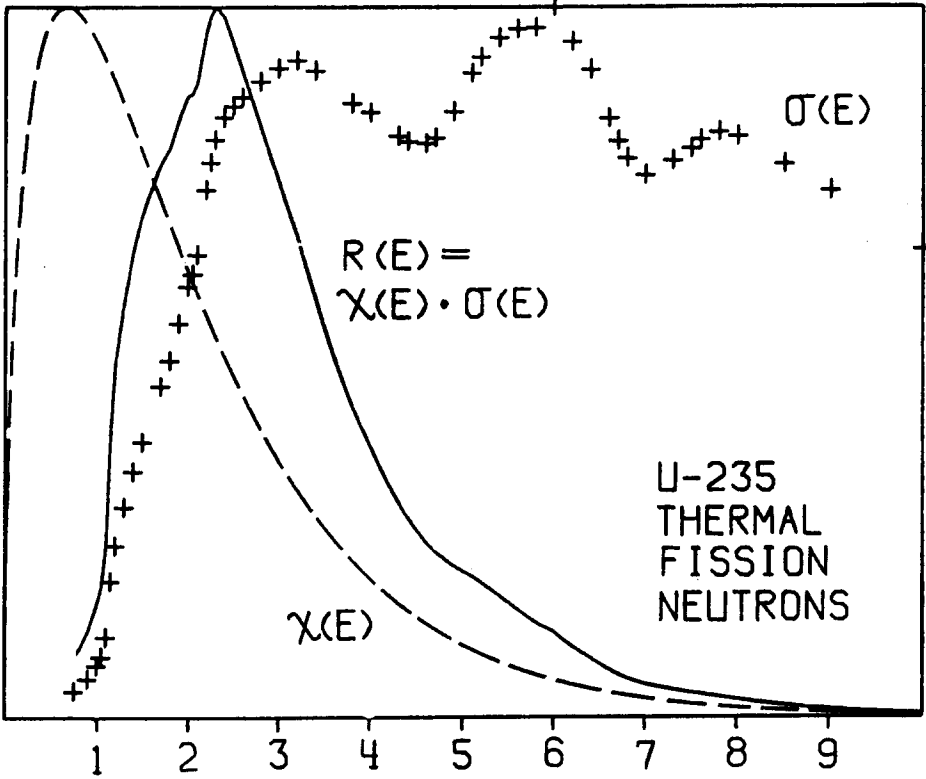


Fig. 8

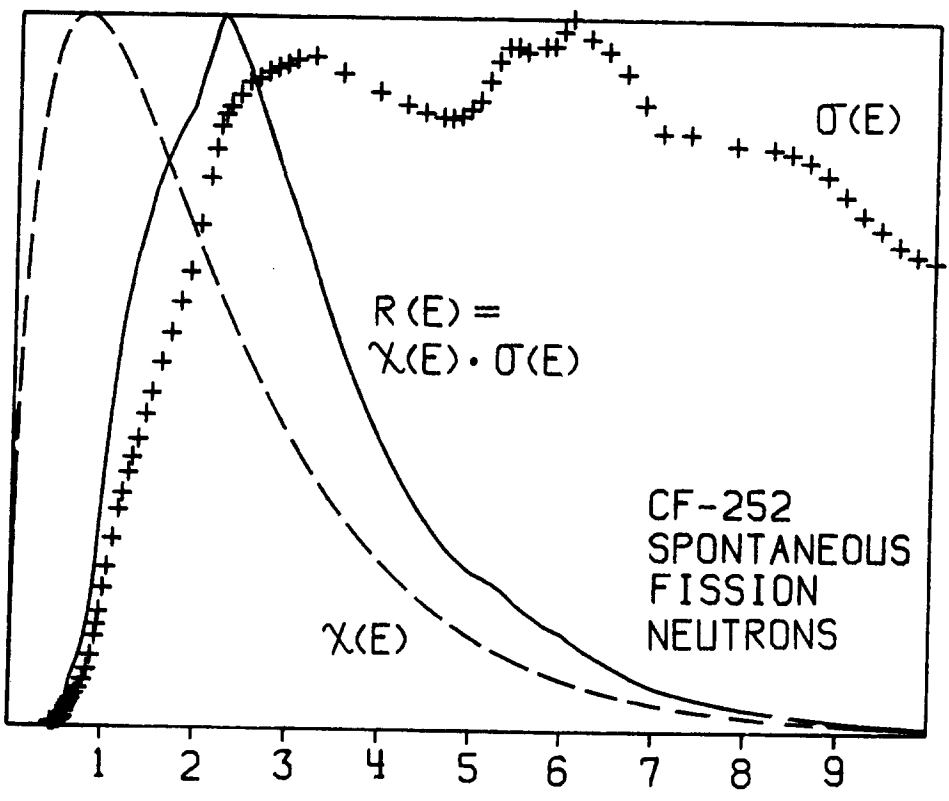
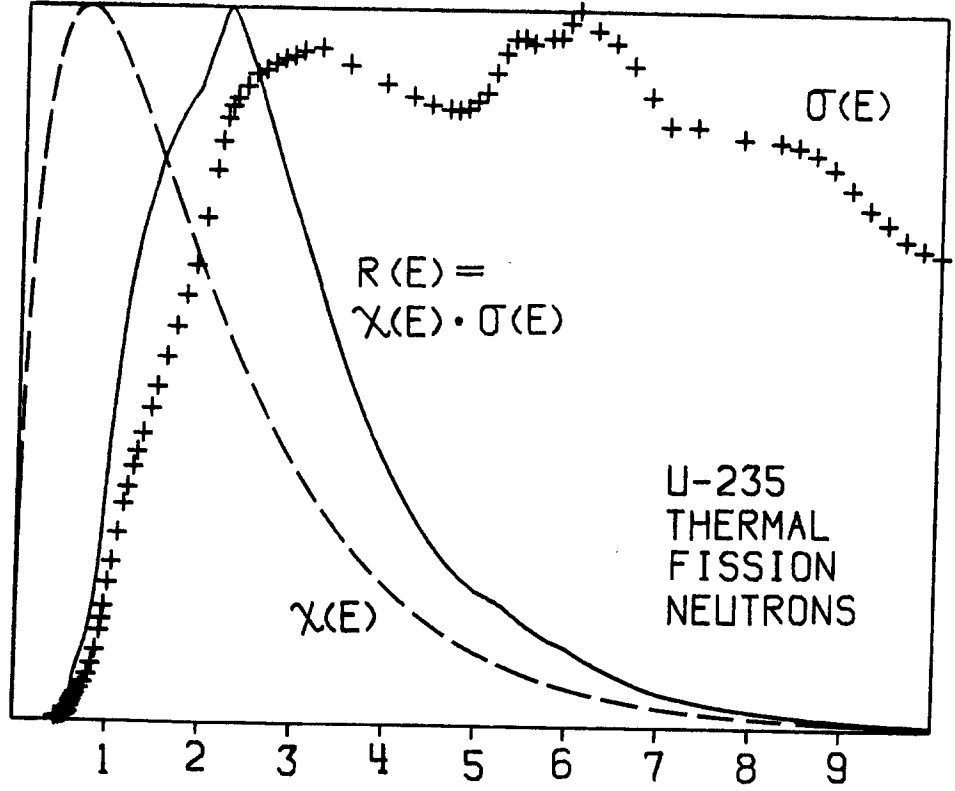
IN-113(N, N') IN-113M

ARBITRARY NORMALIZATION



IN-115 (N, N') IN-115M

ARBITRARY NORMALIZATION



E, MEV